JOURNAL OF COMPUTATIONAL PHYSICS 78, 94–113 (1988)

Open Boundary Conditions for Stationary Inviscid Flow Problems

LARS FERM

Department of Scientific Computing, Uppsala University, Sweden

Received January 8, 1987; revised September 1, 1987

The steady state problem for flow in a channel is considered. Very accurate open upstream and downstream boundary conditions are derived for the Euler equations. No data are needed at the boundaries. It is enough that the upstream limit of the solution is available. Error estimates are derived for a simple model problem, and numerical experiments verify the results for the true non-linear equations. Newton's method is used to solve the equations. The boundary conditions are given in such a form that they also can be used in connection with a time-dependent procedure. © 1988 Academic Press, Inc.

1. INTRODUCTION

An artificial boundary is often introduced when the flow around an object like an airfoil is calculated numerically. Usually no data are available at such a boundary, but data are needed to make the problem well posed. Hence a special kind of boundary conditions is needed, and in this paper very accurate conditions for the steady state Euler equations are constructed. When the boundary conditions are derived, the only approximation is to introduce the free stream values of the solution into the coefficient matrices in the area outside the artificial boundary. The fundamental solution of the constant coefficient problem obtained is constructed. The boundary conditions are designed such that they are satisfied exactly by the fundamental solution. Therefore these conditions will be called the fundamental boundary conditions. Hagstrom and Keller [10, 11] discuss exact boundary conditions from a general point of view but they do not derive any conditions for the Euler equations. The boundary conditions derived here are based on an idea given by Gustafsson and Kreiss [9] for a simple example. The downstream conditions have already been derived by Ferm and Gustafsson [6]. The procedure can also be generalized to the external problem [5]. Exact boundary conditions of a similar type have also been derived for the Helmholz equation by Fix and Marin [7].

Several authors have introduced further approximations in addition to freezing the coefficients. Engquist and Majda [2, 3], and Bayliss and Turkel [1] study the time-dependent problem and obtain conditions from truncated expansions. The first approximation by Engquist and Majda, i.e., using free stream data for the in-going characteristic variables, has often been used in steady state calculations. Obviously

0021-9991/88 $3.00

that requires such a large computational region that the free stream data make good approximations to these characteristic variables at the boundary. Similarly, Bayliss and Tukel [1] suggest an implementation of their boundary condition such that the pressure of the converged solution takes the free stream value at the boundary. So does also the converged pressure obtained with the boundary condition studied by Rudy and Strikwerda in [12]. Engquist and Majda's conditions are derived for constant initial data outside the boundary. The technique has recently been generalized by Gustafsson [8] such that waves coming from the outside are taken into account. His conditions are intended for the time-dependent problem.

For the fundamental conditions two linear combinations of the physical variables are shown to be constant in the free stream direction, i.e., in the direction of the channel. That gives two conditions at every inflow point. Algebraic relations between the Fourier coefficients of the fundamental solution are also used as boundary conditions. Therefore one variable is Fourier transformed along the artificial boundary, and one variable is transformed back to the physical space at every solution step.

The boundary conditions are derived in Section 2. They are given a form such that they can be used in connection with Newton's method or in connection with a time-dependent method. Energy estimates show the well-posedness in Section 3. Section 4 contains an error analysis for a simple model problem, and the results are verified experimentally for the nonlinear problem in Section 5. Some conclusions are given in Section 6.

2. Derivation of the Boundary Conditions

Consider the steady state Euler equations

$$Aw_x + Bw_y = 0, \tag{2.1}$$

where

$$w = \begin{bmatrix} \rho \\ u \\ v \\ p \end{bmatrix}; \quad A = \begin{bmatrix} u & \rho & 0 & 0 \\ 0 & u & 0 & 1/\rho \\ 0 & 0 & u & 0 \\ 0 & c^2\rho & 0 & u \end{bmatrix}; \quad B = \begin{bmatrix} v & 0 & \rho & 0 \\ 0 & v & 0 & 0 \\ 0 & 0 & v & 1/\rho \\ 0 & 0 & c^2\rho & v \end{bmatrix}.$$

The geometry is an infinitely long channel with plane walls outside a bounded region as shown in Fig. 1. We assume that the flow is subsonic and without discontinuities in the far regions F_1 and F_2. The construction of the boundary conditions depends only on the properties outside the artificial boundaries. Thus discontinuities are allowed in the interior of the computational domain. A natural assumption is that the limits of the solution far away from the non-uniform

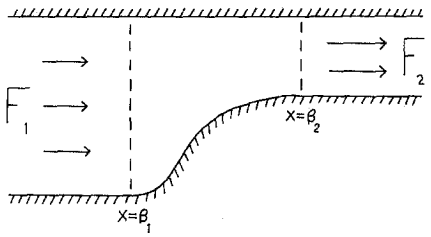

FIG. 1. Flow in a channel.

geometry are constant. We assume that some knowledge about these limits is available. If the upstream limit is known completely, no information is needed about the limit to the right. Note that the limits to the left and to the right are not equal for a problem like that in Fig. 1.

When the boundary conditions are constructed the coefficient matrices are frozen at constant states denoted by $\bar{u}$, $\bar{w}$, $\bar{v}$,... in the far regions F_1 and F_2. The free stream values should be used here, but if they are not available a mean value along the artificial boundary will do. The condition $\bar{v}=0$ will be used since

$$\lim_{|x|\to\infty} v(x, y)=0.$$

The frozen steady state system is

$$\bar{A}w_x+\bar{B}w_y=0, \tag{2.2}$$

where

$$\bar{A}=\begin{bmatrix} \bar{u} & \bar{\rho} & 0 & 0 \\ 0 & \bar{u} & 0 & 1/\bar{\rho} \\ 0 & 0 & \bar{u} & 0 \\ 0 & \bar{c}^2\bar{\rho} & 0 & \bar{u} \end{bmatrix}; \qquad \bar{B}=\begin{bmatrix} 0 & 0 & \bar{\rho} & 0 \\ 0 & 0 & 0 & 0 \\ 0 & 0 & 0 & 1/\bar{\rho} \\ 0 & 0 & \bar{c}^2\bar{\rho} & 0 \end{bmatrix}.$$

The second equation and a linear combination of the first and fourth equation are

$$\frac{d}{dx}[p(x, y)+\bar{\rho}\bar{u}u(x, y)]=0$$

$$\frac{d}{dx}[p(x, y)-\bar{c}^2\rho(x, y)]=0.$$

This leads to the boundary conditions

$$\begin{aligned} p(\beta_1, y)-p_{-\infty}+\bar{\rho}\bar{u}[u(\beta_1, y)-u_{-\infty}]&=0 \\ p(\beta_1, y)-p_{-\infty}-\bar{c}^2[\rho(\beta_1, y)-\rho_{-\infty}]&=0. \end{aligned} \tag{2.3}$$

A system for p and v alone can be derived from the frozen equations (2.2)

$$\begin{bmatrix} v \\ p \end{bmatrix}_x + H \begin{bmatrix} v \\ p \end{bmatrix}_y = 0, \tag{2.4}$$

where

$$H = \begin{bmatrix} 0 & 1/\bar{\rho}\bar{u} \\ -\bar{c}^2\bar{\rho}\bar{u}/\bar{r}^2 & 0 \end{bmatrix}$$

$$\bar{r} = \sqrt{\bar{c}^2 - \bar{u}^2}.$$

Since $p_y = v = 0$ at the channel walls $y = 0$ and $y = 1$, the expansions

$$\begin{aligned} v(x, y) &= \sum_{\omega=1}^{\infty} \hat{v}_\omega(x) \sin \pi\omega y \\ p(x, y) &= \sum_{\omega=0}^{\infty} \hat{p}_\omega(x) \cos \pi\omega y \end{aligned} \tag{2.5}$$

are well suited for this problem. We introduce these expansions into the system (2.4), and get

$$\frac{d}{dx}\begin{bmatrix} \hat{v}_\omega \\ \hat{p}_\omega \end{bmatrix} + \omega\pi\hat{H}\begin{bmatrix} \hat{v}_\omega \\ \hat{p}_\omega \end{bmatrix} = 0, \qquad \omega = 1, 2, \ldots, \tag{2.6a}$$

$$\frac{d}{dx}\hat{p}_0(x) = 0, \tag{2.6b}$$

where

$$\hat{H} = \begin{bmatrix} 0 & -1/\bar{\rho}\bar{u} \\ -\bar{c}^2\bar{\rho}\bar{u}/\bar{r}^2 & 0 \end{bmatrix}. \tag{2.7}$$

The general solution of this problem has the form

$$\begin{bmatrix} \hat{v}_\omega \\ \hat{p}_\omega \end{bmatrix} = \alpha_1 q_1 e^{\lambda_1 x} + \alpha_2 q_2 e^{\lambda_2 x}, \tag{2.8}$$

where q_i and λ_i are the solutions of the eigenvalue problem

$$(\lambda_i I + \omega\pi\hat{H})\, q_i = 0. \tag{2.9}$$

A simple calculation shows that

$$\lambda_1 = -\lambda_2 = \frac{c\omega\pi}{\bar{r}}; \qquad q_1 = \begin{bmatrix} \bar{r} \\ \bar{c}\bar{\rho}\bar{u} \end{bmatrix}; \qquad q_2 = \begin{bmatrix} -\bar{r} \\ \bar{c}\bar{\rho}\bar{u} \end{bmatrix}. \tag{2.10}$$

In the downstream far region the coefficient α_1 must be zero for $\omega \neq 0$, otherwise the solution is unbounded. The ratio between the elements of q_2 leads to the downstream boundary condition

$$\hat{p}_\omega(\beta_2) = -\frac{\bar{c}\bar{\rho}\bar{u}}{\bar{r}}\hat{v}_\omega(\beta_2), \qquad \omega = 1, 2, \ldots . \tag{2.11}$$

Similarly α_2 is zero in the upstream far region, and we get

$$\hat{v}_\omega(\beta_1) = \frac{\bar{r}}{\bar{c}\bar{\rho}\bar{u}}\hat{p}_\omega(\beta_1), \qquad \omega = 1, 2, \ldots . \tag{2.12}$$

Equation (2.6b) gives the downstream condition

$$\hat{p}_0(\beta_2) = p_\infty . \tag{2.13}$$

The boundary conditions (2.3), (2.11), (2.12), (2.13) form a complete set of conditions for the differential equations. They can be implemented in different ways in a practical calculation. A simple procedure is to multiply the downstream conditions (2.11), (2.13) by $\cos \pi\omega y$. Summation over ω yields

$$p(\beta_2, y) = p_\infty - \frac{\bar{c}\bar{\rho}\bar{u}}{\bar{r}} \sum_{\omega=1}^{\infty} \hat{v}_\omega(\beta_2) \cos \pi\omega y. \tag{2.14a}$$

The corresponding upstream condition is

$$v(\beta_1, y) = \frac{\bar{r}}{\bar{c}\bar{\rho}\bar{u}} \sum_{\omega=1}^{\infty} \hat{p}_\omega(\beta_1) \sin \omega\pi y. \tag{2.14b}$$

A large number of experiments have been carried out where the derivatives are approximated by central differences in the computational domain, and the resulting system of algebraic equations is solved using Newton's method. The true Jacobian has been used. Extrapolations of p from the interior to the upstream boundary, and of ρ, u, v to the downstream boundary work well in connection with Newton's method.

The condition (2.13) entering in the condition (2.14a) cannot be applied if no downstream data are available. Consider the mass flow per unit time

$$m(x) = \int_{\substack{\text{across} \\ \text{the channel}}} \rho(x, y)\, u(x, y)\, dy.$$

It is easily shown that $m(x)$ is independent of x for the true non-linear equations even if the channel walls are not planes. Thus an exact boundary condition is given by

$$m(\beta_2) = \lim_{x \to -\infty} m(x).$$

However, some care must be observed when this condition is used in connection with a time-marching procedure in the interior. Consider the corresponding linearized homogeneous boundary condition

$$\bar{\rho}\hat{u}_0(\beta_2) + \bar{u}\hat{\rho}_0(\beta_2) = 0, \tag{2.15}$$

and the Fourier transformed homogeneous upstream conditions (2.3) for $\omega = 0$, i.e.,

$$\hat{p}_0(\beta_1) - \bar{\rho}\bar{u}\hat{u}_0(\beta_1) = \hat{p}_0(\beta_1) - \bar{c}^2\hat{\rho}_0(\beta_1) = 0.$$

Usual Laplace transform analysis shows that this combination of upstream and downstream conditions leads to increasing solutions of the time-dependent equations.

Therefore we will modify the boundary conditions and subtract the conditions (2.3) by their Fourier transformed versions for $\omega = 0$. Now two scalar constants are missing at the upstream boundary. Delete the third of the frozen equations (2.2), and integrate the remaining system across the channel. That yields

$$\frac{d}{dx}\hat{\rho}_0(x) = \frac{d}{dx}\hat{u}_0(x) = \frac{d}{dx}\hat{p}_0(x) = 0,$$

where $\hat{\rho}_0(x) = \int_0^1 \rho(x, y)\, dy$, etc.

Thus the mean values across the channel of ρ, u, p are independent of x in the far regions outside the artificial boundaries. Knowledge of the left free stream data thus leads to accurate values for three scalar constants at the upstream boundary. Only two values are needed, and a natual choice for rapid convergence to the steady state is the two in-going characteristic variables containing ρ, u, p. For time-dependent procedures that is the most efficient treatment of the mean-values that has been tested. Well-posedness will be shown in Section 3. The out-going characteristic variables have been extrapolated from the interior to the boundary in calculations with time-dependent procedures.

In connection with Newton's method the conditions for $\omega = 0$ have shown less influence on the convergence rate to the steady state. For example the instability mentioned above for time-dependent methods has not turned up with Newton's method. Extrapolations from the interior of physical variables and characteristic variables have been used in calculations with Newton's method. The following complete set of boundary conditions work well in connection with time-dependent procedures and also in connection with Newton's method:

1. the conditions (2.14) for ω greater than zero,

$$p(\beta_2, y) - \hat{p}_0(\beta_2) = -\frac{\bar{c}\bar{\rho}\bar{u}}{\bar{r}} \sum_{\omega=1}^{\infty} \hat{v}_\omega(\beta_2) \cos \pi\omega y \tag{2.16a}$$

$$v(\beta_1, y) = \frac{\bar{r}}{\bar{c}\bar{\rho}\bar{u}} \sum_{\omega=1}^{\infty} \hat{p}_\omega(\beta_1) \sin \pi\omega y; \tag{2.16b}$$

2. the conditions (2.3) for ω greater than zero,

$$p(\beta_1, y) - \hat{p}_0(\beta_1) + \bar{\rho}\bar{u}[u(\beta_1, y) - \hat{u}_0(\beta_1)] = 0 \tag{2.17a}$$

$$p(\beta_1, y) - \hat{p}_0(\beta_1) - \bar{c}^2[\rho(\beta_1, y) - \hat{\rho}_0(\beta_1)] = 0; \tag{2.17b}$$

3. the upstream conditions when ω is zero

$$\bar{c}^2\hat{\rho}_0(\beta_1) - \hat{p}_0(\beta_1) = \bar{c}^2\rho_{-\infty} - p_{-\infty} \tag{2.18a}$$

$$\bar{\rho}\bar{c}\hat{u}_0(\beta_1) + \hat{p}_0(\beta_1) = \bar{\rho}\bar{c}u_{-\infty} + p_{-\infty}; \tag{2.18b}$$

4. the downstream condition when ω is zero: use one of the conditions

$$\bar{\rho}\bar{c}\hat{u}_0(\beta_2) - \hat{p}_0(\beta_2) = \bar{\rho}\bar{c}u_{\infty} - p_{\infty} \tag{2.19a}$$

$$\hat{p}_0(\beta_2) = p_{\infty} \tag{2.19b}$$

$$m(\beta_2) = \lim_{x \to -\infty} m(x). \tag{2.19c}$$

Remark 1. When the limit at infinity depends on y, the right-hand sides of (2.17) are not zero and the mean values at infinity are used in (2.18), (2.19).

Remark 2. In connection with Newton's method the conditions (2.17)–(2.18) can be replaced by the unmodified conditions (2.3) for simplicity.

Remark 3. A simple procedure applicable in connection with Newton's method when only upstream data are available, is to specify all three required mean values $\hat{\rho}_0$, $\hat{u}_0$, $\hat{p}_0$ at the upstream boundary. A value from the interior is used for $\hat{p}_0$ at the downstream boundary. Only a few calculations have been carried out with this procedure, but they all worked well. In these calculations $p(x, y) - \hat{p}_0(x)$ was extrapolated from the interior to the upstream boundary.

Remark 4. In connection with a time-dependent procedure condition (2.19a) leads to the most rapid convergence to the steady state. Conditions (2.19b) and (2.19c) can be used if u_{∞} or p_{∞} are not available. Note that condition (2.19c) makes use of upstream data at the downstream boundary.

Remark 5. Assume that a linear combination of p and u at the upstream boundary is obtained directly from the calculations in the interior (for example, via extrapolations). Then p and u can be calculated locally using the boundary conditions (2.17a), (2.18b). When p is Fourier transformed along the boundary, v is obtained from condition (2.16b). The downstream boundary is treated similarly.

Remark 6. In connection with an explicit method condition (2.19c) usually leads to a second-degree equation for one of the mean values. If u or ρ is determined from the other conditions the equation is linear. In connection with Newton's method condition (2.19c) can be treated implicitly (see [6]).

Remark 7. In the isentropic case the equations

$$p_x = \bar{c}^2 \rho_x,$$
$$p_y = \bar{c}^2 \rho_y$$

lead to the conditions

$$\hat{p}_\omega = \bar{c}^2 \hat{\rho}_\omega, \qquad \omega > 0.$$

Note that the second differential equation leading to conditions (2.3), and hence condition (2.17b), becomes meaningless.

The Semi-discretized Channel Problem

This is given by

$$Aw_x + BD_y w = 0, \tag{2.20}$$

where

$$D_y w(x, y_l) = \begin{cases} D_{+y} w(x, y_l) & \text{for } l = 0 \\ D_{0y} w(x, y_l) & \text{for } l = 1, ..., M-1 \\ D_{-y} w(x, y_l) & \text{for } l = M \end{cases}$$

$$y_l = \frac{l}{M}, \qquad l = 0, 1, ..., M$$

$$v(x, 0) = v(x, 1) = 0.$$

The fundamental boundary conditions for this problem can be shown to be identical to those of the differential equations. The proof is analogous. Note that the semi-discretized equations corresponding to (2.4) can be Fourier transformed using the finite expansions corresponding to (2.5).

Flow in a Periodic Channel

Assume that the solution is periodic on the η-direction, and that the (ζ, η)-coordinate system is obtained by a rotation of the (x, y)-system. Assume also that the x-axis is parallel to the free stream direction, and that u and v are the velocity components in the x- and y-directions. The artificial boundaries are given by $\zeta = \beta_1$ and $\zeta = \beta_2$. When the steady state Euler equations are frozen around the free stream values, we get

$$\bar{A} w_x + \bar{B} w_y = 0,$$

where the diagonal of $\bar{B}$ is zero since $\bar{v} = v_\infty = 0$. This leads to the extrapolations (2.3) across the far region and to the system (2.4) for p and v. To solve (2.4) we rotate the coordinate system into the (ζ, η)-system without changing the dependent

variables. Assuming that the period length is 2π, the resulting equations can be solved using the Fourier expansions

$$\begin{bmatrix} p(\zeta,\eta) \\ v(\zeta,\eta) \end{bmatrix} = \sum_{\omega=0}^{\infty} \begin{bmatrix} \hat{p}_c(\zeta,\omega) \\ \hat{v}_c(\zeta,\omega) \end{bmatrix} \cos\omega\eta + \sum_{\omega=1}^{\infty} \begin{bmatrix} \hat{p}_s(\zeta,\omega) \\ \hat{v}_s(\zeta,\omega) \end{bmatrix} \sin\omega\eta. \tag{2.21}$$

Some calculation leads to the downstream boundary conditions

$$\begin{aligned} \hat{p}_s(\zeta,\omega) &= \frac{\bar{c}\bar{\rho}\bar{u}}{\bar{r}}\hat{v}_c(\zeta,\omega) \\ \hat{p}_c(\zeta,\omega) &= -\frac{\bar{c}\bar{\rho}\bar{u}}{\bar{r}}\hat{v}_s(\zeta,\omega). \end{aligned} \tag{2.22}$$

At the upstream boundary the signs on one side of the equal signs are reversed. Note that v as in the channel problem is the velocity component in the direction perpendicular to the free stream direction. The fundamental boundary conditions for the incompressible periodic channel problem have been studied in [4].

3. Energy Estimates for Time-Dependent Methods

The channel problem studied here is solved very efficiently using Newton's method but steady state problems are often solved using time-dependent procedures. In this section it is shown that conditions (2.16)–(2.19) lead to well-posed problems for the constant coefficient unsteady differential equations.

Consider the time-dependent system corresponding to (2.2) in the interior region. The Fourier expansions (2.5), and the corresponding cosine-expansions of u and ρ lead to the Fourier transformed system

$$\frac{\partial}{\partial t}\tilde{w}_\omega + \Lambda\frac{\partial}{\partial x}\tilde{w}_\omega + \omega\pi\frac{\bar{c}}{\sqrt{2}}\tilde{B}\tilde{w}_\omega = 0, \tag{3.1}$$

where

$$\tilde{w}_\omega = \begin{bmatrix} \tilde{\rho}_\omega \\ \tilde{u}_\omega \\ \tilde{v}_\omega \\ \tilde{p}_\omega \end{bmatrix} = S^{-1}\begin{bmatrix} \hat{\rho}_\omega \\ \hat{u}_\omega \\ \hat{v}_\omega \\ \hat{p}_\omega \end{bmatrix}; \qquad S = \begin{bmatrix} 1 & \bar{\rho} & 0 & \bar{\rho} \\ 0 & \bar{c} & 0 & -\bar{c} \\ 0 & 0 & \bar{c}\sqrt{2} & 0 \\ 0 & \bar{c}^2\bar{\rho} & 0 & \bar{c}^2\bar{\rho} \end{bmatrix}, \tag{3.2}$$

$$\Lambda = \operatorname{diag}(\bar{u}, \bar{u}+\bar{c}, \bar{u}, \bar{u}-\bar{c}); \qquad \tilde{B} = \begin{bmatrix} 0 & 0 & 0 & 0 \\ 0 & 0 & 1 & 0 \\ 0 & -1 & 0 & -1 \\ 0 & 0 & 1 & 0 \end{bmatrix},$$

$\hat{\rho}_\omega$, $\hat{u}_\omega$, $\hat{v}_\omega$, $\hat{p}_\omega$ are the Fourier coefficients of ρ, u, v, p; respectively, $\tilde{\rho}_\omega$, $\tilde{u}_\omega$, $\tilde{v}_\omega$, $\tilde{p}_\omega$ are the Fourier transformed characteristic variables in the x-direction. Introduce the norm

$$\|\tilde{w}_\omega\|^2 = (\tilde{w}_\omega, \tilde{w}_\omega) = \int_{\beta_1}^{\beta_2} (\tilde{\rho}_\omega^2 + \tilde{u}_\omega^2 + \tilde{v}_\omega^2 + \alpha\tilde{p}_\omega^2)\, dx,$$

where α is a parameter greater than zero. Using the differential equations (3.1), we get

$$\frac{d}{dt}\|\tilde{w}_\omega\|^2 = E(\beta_2) - E(\beta_1) - 2\omega\pi \frac{\bar{c}}{\sqrt{2}} (\tilde{B}\tilde{w}_\omega, \tilde{w}_\omega), \tag{3.3}$$

where

$$E(x) = -\bar{u}\tilde{\rho}_\omega(x)^2 - (\bar{c} + \bar{u})\, \tilde{u}_\omega(x)^2 - \bar{u}\tilde{v}_\omega(x)^2 + \alpha(\bar{c} - \bar{u})\, \tilde{p}_\omega(x)^2.$$

Consider $\omega \neq 0$, and set the parameter α equal to one. The last term of (3.3) is zero since $\tilde{B}$ is skew-symmetric. The upstream boundary conditions corresponding to (2.16b) and (2.17) are

$$\tilde{\rho}_\omega(\beta_1) = 0$$

$$\tilde{u}_\omega(\beta_1) = -\frac{\bar{c} - \bar{u}}{\bar{c} + \bar{u}}\, \tilde{p}_\omega(\beta_1)$$

$$\tilde{v}_\omega(\beta_1) = \frac{\bar{r}}{\bar{u}\sqrt{2}} [\tilde{u}_\omega(\beta_1) + \tilde{p}_\omega(\omega_1)].$$

When these conditions are introduced into (3.3), we get

$$E(\beta_1) = 0.$$

$$\tilde{p}_\omega(\beta_2) = -\tilde{u}_\omega(\beta_2) - u\frac{\times}{\bar{r}}\, \tilde{v}_\omega(\beta_2),$$

which leads to

$$\begin{aligned} E(\beta_2) &= -\bar{u}\tilde{\rho}_\omega(\beta_2)^2 \\ &\quad + \bar{u}\left\{-2\tilde{u}_\omega(\beta_2)^2 - \frac{\bar{c} - \bar{u}}{\bar{c} + \bar{u}}\, \tilde{v}_\omega(\beta_2)^2 + 2\sqrt{2\frac{\bar{c} - \bar{u}}{\bar{c} + \bar{u}}}\, \tilde{v}(\beta_2)\, \tilde{u}(\beta_2)\right\} \\ &= -\bar{u}\tilde{\rho}_\omega(\beta_2)^2 - \bar{u}\left\{\sqrt{2}\, \tilde{u}_\beta(\beta_2) - \sqrt{\frac{\bar{c} - \bar{u}}{\bar{c} + \bar{u}}}\, \tilde{v}_\omega(\beta_2)\right\}^2 \leqslant 0. \end{aligned}$$

It remains to obtain estimates when ω is zero. The last term of (3.3) is zero even when the parameter α is not equal to one. Since v is expanded in a sine series, there exists no Fourier coefficient $\hat{v}_0$. Thus the variable $\tilde{v}_0$ defined by (3.2) is deleted in (3.3). The homogeneous upstream boundary conditions corresponding to (2.18) are

$$\tilde{\rho}_0(\beta_1) = \tilde{u}_0(\beta_1) = 0,$$

which yields

$$E(\beta_1) = \alpha(\bar{c} - \bar{u})\, \tilde{p}_\omega(\beta_1)^2.$$

Thus the upstream boundary terms of (3.3) are always less than or equal to zero. The downstream conditions corresponding to (2.19) are

$$\begin{aligned} &\tilde{p}_0(\beta_2) = 0 \\ &\tilde{p}_0(\beta_2) = -\tilde{u}_0(\beta_2) \\ &\tilde{p}_0(\beta_2) = \frac{\bar{u}}{\bar{\rho}(\bar{c} - \bar{u})}\, \tilde{\rho}_0(\beta_2) + \frac{\bar{c} + \bar{u}}{\bar{c} - \bar{u}}\, \tilde{u}_0(\beta_2). \end{aligned} \tag{3.4}$$

The last condition is equivalent to condition (2.15).

When $\tilde{p}_0(\beta_2)$ is eliminated by one of the conditions (3.4), $E(\beta_2)$ becomes a quadratic form in $\tilde{u}_0(\beta_2)$ and $\tilde{\rho}_0(\beta_2)$. It is obvious that if the parameter α is chosen small enough, this quadratic form is less than or equal to zero independently of $\tilde{u}_0(\beta_2)$ and $\tilde{\rho}_0(\beta_2)$.

The estimates derived above lead to

$$\frac{d}{dt} \|\tilde{w}_\omega\|^2 \leqslant 0, \qquad \omega = 0, 1, 2, \ldots .$$

Thus the linearized time-dependent problem with the boundary conditions (2.16)–(2.19) is well posed.

4. Error Analysis

Consider the following simple model problem with constant coefficients:

$$\begin{aligned} &A_0 w_x^{(T)} + B_0 w_y^{(T)} = 0, \qquad 0 \leqslant x < \infty, \quad 0 \leqslant y \leqslant 1 \\ &w_1^{(T)}(0, y) = g(y) \\ &\lim_{x \to \infty} p^{(T)}(x, y) = p_\infty \\ &v^{(T)}(x, 0) = v^{(T)}(x, 1) = 0. \end{aligned} \tag{4.1}$$

Here

$$\begin{matrix} A_0 = A(w_0) \\ B_0 = B(w_0) \end{matrix}, \qquad w_0 = \begin{bmatrix} \rho_0 \\ u_0 \\ v_0 \\ p_0 \end{bmatrix},$$

$$w_1 = \begin{bmatrix} \rho \\ u \\ v \end{bmatrix}, \qquad g(y) = \begin{bmatrix} g_1(y) \\ g_2(y) \\ g_3(y) \end{bmatrix}.$$

Functions $g_i(y)$ are specified and w_0 is constant with $v_0 = 0$.

This problem can be solved using the technique in Section 2, and the fundamental boundary conditions lead to the correct solution if the region is truncated at an artificial boundary $x = \beta > 0$. However, if we use $\bar{u} \neq u_0$, $\bar{\rho} \neq \rho_0$, etc., in the boundary condition, i.e., change the coefficient matrices in the area $x > \beta$, the fundamental conditions will usually not lead to exactly the correct solution. The error obtained can be expected to give an idea of the error when the fundamental conditions are used for the non-linear problem. In that case the change of the matrices is due to the freezing of the coefficient matrices in the far region. Denote the solution of the model problem (4.1) by $w^{(T)}$, and the solution of the truncated problem with the fundamental boundary conditions (2.16a), (2.19b) by $w^{(F)}$. Straightforward calculation leads to the estimate

$$\|w^{(T)}(x, \cdot) - w^{(F)}(x, \cdot)\| \sim \delta \, \|v^{(T)}(\beta, \cdot)\|, \tag{4.2}$$

where

$$\delta = \left| \frac{c_0 \rho_0 u_0 \bar{r}}{\bar{c}\bar{\rho}\bar{u}r_0} - 1 \right|.$$

The factor δ depends on the change of the matrices. For the non-linear problem that change varies in the far region, and we estimate δ by

$$\delta \sim \delta_x + \delta_y,$$

where

$$\delta_x = \max_{x_i > \beta} |w(x_1, y) - w(x_2, y)|$$

$$\delta_y = \max_{y_1, y_2} |w_\infty(y_1) - w_\infty(y_2)|.$$

The linear analysis leads to

$$\delta_x \sim \|v(\beta, \cdot)\|,$$

and we get the final estimate

$$\|w^{(T)}(x,\cdot)-w^{(F)}(x,\cdot)\| \sim \|v^{(T)}(\beta,\cdot)\|^2+\delta_y\|v^{(T)}(\beta,\cdot)\|. \tag{4.3}$$

Note that δ_y is zero in the natural case when the limit at infinity is independent of y. Note also that

$$\lim_{x\to\infty}\|v^{(T)}(\beta,\cdot)\|=0.$$

For comparison we also solve the truncated problem when the pressure is set to the free stream value at the boundary. The solution is denoted by $w^{(I)}$. Some calculation leads to the estimate

$$\|w^{(T)}(x,\cdot)-w^{(I)}(x,\cdot)\| \sim \|v^{(T)}(\beta,\cdot)\|. \tag{4.4}$$

A comparison between the estimates (4.3) and (4.4) demonstrates the higher order of accuracy of the fundamental boundary conditions in the natural case when δ_y is zero.

The upstream open boundary problem corresponding to the downstream open boundary problem (4.1) is

$$\begin{gathered} A_0 w_x + B_0 w_y = 0, \qquad -\infty < x \leqslant 0, \quad 0 \leqslant y \leqslant 1 \\ \lim_{x\to-\infty} w_1(x,y) = g(y) \\ p(0,y) = f(y) \\ v(x,0) = v(x,1) = 0, \end{gathered} \tag{4.5}$$

where

$$g(y)=\begin{bmatrix} g_1(y) \\ g_2(y) \\ 0 \end{bmatrix}$$

and $f(y)$ are given functions.

When the artificial boundary $x=-\beta$ is introduced, analogous calculations lead to the same error estimates as for the downstream open boundary problem.

5. Numerical Experiments

The constant coefficient error estimates given in the preceding section are verified for the true non-linear equations by experiments presented in this section. The derivatives are approximated by central differences and the resulting systems of algebraic equations are solved directly using Newton's method.

Since the fundamental boundary conditions are very accurate a fine mesh is needed to make the errors due to the boundary conditions dominate but it turns out that it is only necessary to refine the mesh in the x-direction. Even when the mesh is coarse in the y-direction, the solution is changed very little when the artificial boundary is moved along the channel. The errors due to the difference approximations in the area between the different artificial boundaries seem to disappear. The explanation is that the fundamental boundary conditions for the semi-discretized problem (2.20) are exactly the same as those of the differential equations. It is easily shown that the error estimates also are the same. If the error estimates are verified for the semi-discretized problem, it is just a matter of mesh refinement to transfer the results to the differential equations. That saves much computer capacity since the computational work grows rapidly with the number of grid points across the channel.

EXPERIMENT 1. The half channel problems studied in Section 4 are considered for the isentropic flow when p is eliminated from the system by

$$p = a\rho^{\gamma}, \qquad a = 1.43, \qquad \gamma = 1.4.$$

The reduced system requires a few modifications of the model problems (4.1) and (4.5):

1. The matrices A_0, B_0 are replaced by the corresponding reduced nonlinear matrices.
2. ρ is deleted from the vector w_1.
3. Data for p are replaced by data for ρ.

Note that these model problems determine the treatment of $\omega = 0$ in the boundary conditions.

Second-order extrapolations from the interior are used for u and v at the downstream boundary and for ρ at the upstream boundary. It turns out that the solutions at $x = \pm 1$ are very close to the limits at infinity. Thus the solutions obtained with the artificial boundaries $x = \pm 1$ are very accurate. These accurate solutions are compared to those obtained using $\beta = \pm 0.5$, $\beta = \pm 0.25$, $\beta = \pm 0.1$, and $\beta = \pm 0.05$. To make sure that the errors at the boundary dominate, a 100×15 grid is used over the large region. The grids over the smaller regions coincide with that over the large region. The errors obtained in the experiments are compared to the linear error terms leading to the error estimate (4.2). When values from the non-linear matrices replace w_0 in the definition of δ, this factor becomes variable. Consider the mean value

$$\bar{\delta} = \int_{\beta}^{1} \|\delta(x, \cdot)\|_{L_2} \max_{y} |v(x, y)| \, dx \Big/ \int_{\beta}^{1} \max_{y} |v| \, dx. \tag{5.1}$$

The mean value is weighted since we expect that the freezing of the matrices has a

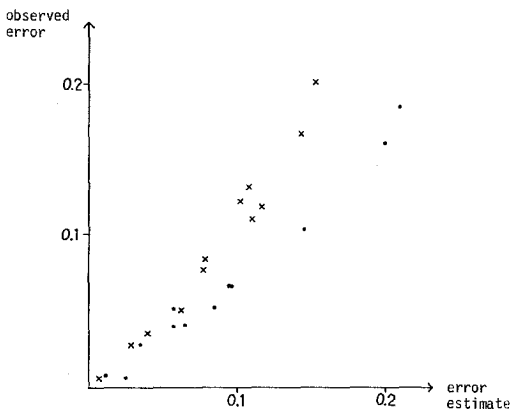

FIG. 2. Test of the linear error estimates: x = the upstream open boundary problem; $\cdot$ = the downstream open boundary problem.

smaller effect far out where the solution is close to the limit at infinity. The results of the experiments are shown in Fig. 2. Every point in the figure represents one experiment. The error estimate is labeled on the x-axis, and the error observed is labeled on the y-axis. Obviously the linear analysis gives a very good picture of the error for the non-linear problem. We also check the more practical error estimate (4.3). Consider the natural case when the limit at infinity is independent of y. Such solutions of the upstream open boundary problem (4.5) can be obtained by choosing constant functions $g_i(y)$. Since the constant δ_y in the error estimate is zero, it is enough to check that δ defined by (5.1) is proportional to $\|v(\beta, \cdot)\|$. The results shown in Fig. 3 confirms that.

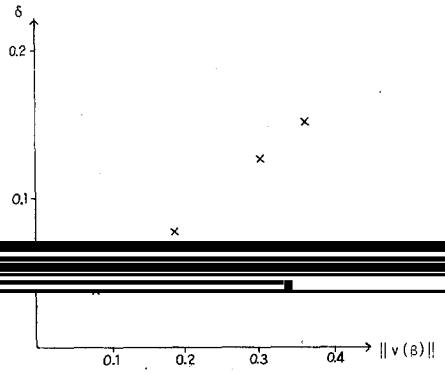

FIG. 3. The factor δ defined by (5.1) as a function of $\|v(\beta)\| = \max_y |v(\beta, y)|$ when the solution at infinity is independent of y.

EXPERIMENT 2. Consider the same half-channel problems when all four variables ρ, u, v, p are involved. The speed of sound is defined by

$$c^2 = \frac{\gamma p}{\rho}.$$

As above, an accurate solution is obtained over an interval of length one, but the grid is only 25×10. The solution of the upstream open boundary problem is shown in Fig. 4. The long curves represent the accurate solution obtained over the long interval. The short curves represent the solution obtained over the small region $-0.2 \leqslant x \leqslant 0$. The curves labeled F are obtained using the fundamental boundary conditions, and those labeled I are obtained using the values at infinity directly at the boundary, i.e.,

$$\rho(-0.2, y) = \rho_{-\infty} = 2.0$$
$$u(-0.2, y) = -\infty = 0.6$$
$$v(-0.2, y) = v_{-\infty} = 0.0.$$

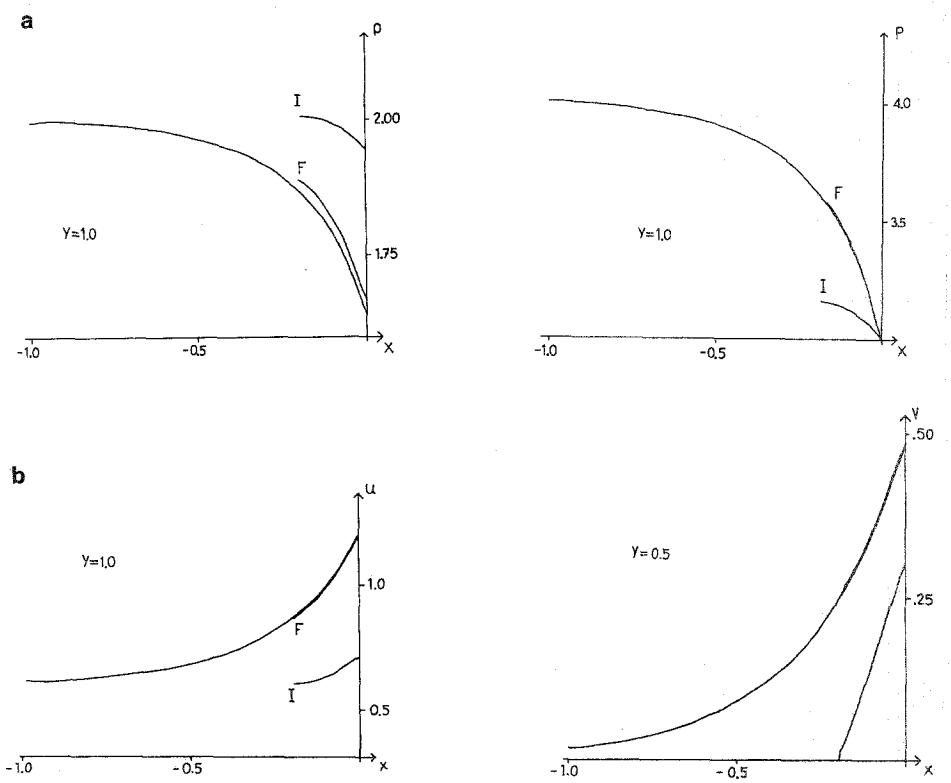

FIG. 4. The upstream open boundary problem.

The data at the fixed downstream boundary is

$$p(0, y) = 4.0 + 0.5 \cos \pi y.$$

The difference in accuracy between the F- and I-solutions is striking. This high accuracy of the fundamental boundary conditions is obtained in the natural case when the limit at infinity is independent of y such that the constant δ_y in the error estimate (4.3) is zero. That the accuracy of the fundamental boundary conditions is worse when the limit at infinity is not constant can be demonstrated by the downstream open boundary problem (4.1) with the data

$$\rho(0, y) = 1.7$$
$$u(0, y) = 0.6$$
$$v(0, y) = 0.5 \sin \pi y$$
$$p_\infty = 3.7.$$

Figure 5a, where the velocity component u is plotted over the region $0 < x < 1$, $0 < y < 1$, shows that the limit to the right of the solution is far from constant. Figure 5b shows a much larger error for the F-conditions than in the preceding experiment, but the F-solution is still more accurate than the I-solution obtained with the boundary condition $p(0.2, y) = p_\infty = 3.7$.

EXPERIMENT 3. Figure 6 shows a problem with two open boundaries. The elevation of the lower channel wall is defined by a sine curve in the interval $|x| < 0.2$. The line $y = 0.5$ can also be regarded as a line of symmetry. In that case

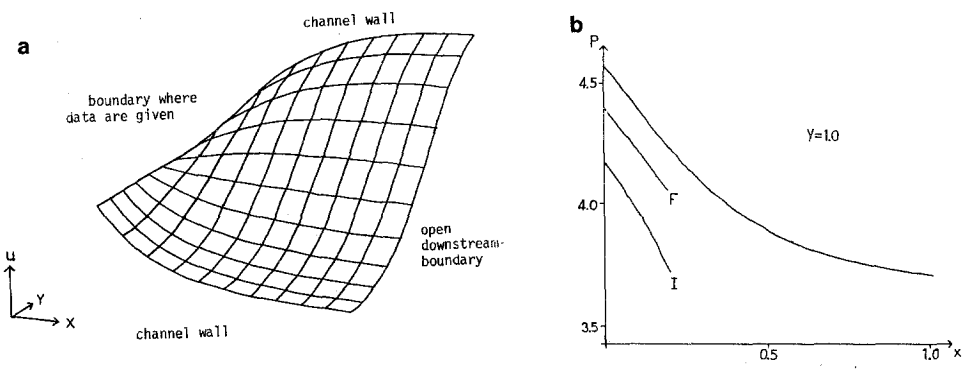

FIG. 5. (a) A solution with y-dependent limit at infinity. (b) The accuracy when the limit at infinity depends on y.

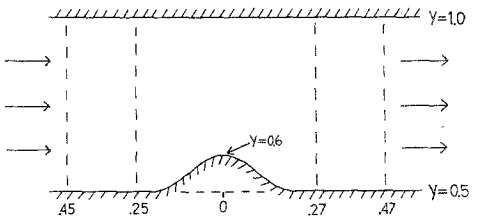

FIG. 6. The model problem.

there is a solid body in the flow. The condition that the velocity component in the normal direction is zero at the channel walls can be written

$$\eta'_x = \frac{v}{u}$$

if the channel wall is given by $y = \eta(x)$.

This condition leads to a discontinuity of the derivatives of the solution at $x = \pm 0.2$ since η''_{xx} is discontinuous there. The transformation

$$\tilde{x} = x$$

$$\tilde{y} = \frac{y - \eta(x)}{1 - \eta(x)}$$

makes the computational region rectangular. The differential equations are transformed into

$$Aw_x + \frac{1}{1-\eta(x)}\left[\eta'(x)(\tilde{y}-1)A + B\right] w_{\tilde{y}} = 0.$$

The data at infinity are

$$u_{-\infty} = 0.6$$

$$\rho_\infty = 2.0.$$

The flow is isentropic and p is eliminated from the system as above. An accurate solution $w^{(T)}$ is obtained over the large region defined by $-0.45 \leqslant x \leqslant 0.47$. The solution $w^{(F)}$ is obtained over the small region $-0.25 \leqslant x \leqslant 0.27$ using the fundamental boundary conditions. The difference $\rho^{(F)} - \rho^{(T)}$ along the channel wall with the elevation is labeled F in Fig. 7. The difference is obviously almost equal to zero. When the values at infinity are used directly as they are for the physical variables at the boundaries, i.e.,

$$u(-0.25, y) = u_{-\infty} = 0.6$$

$$v(-0.25, y) = v_{-\infty} = 0.0$$

$$\rho(0.27, y) = \rho_\infty = 2.0,$$

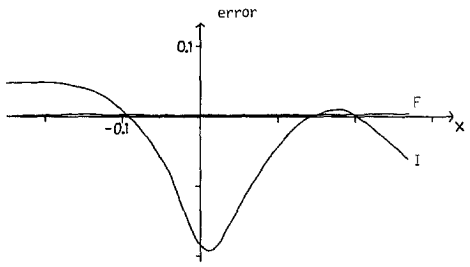

FIG. 7. For the problem with a solid body in the flow, the accuracy of the F-conditions is striking. The errors are plotted along the curve composed of the line of symmetry and the surface of the body.

the solution does not converge even if $w^{(T)}$ is used as the initial solution. The solution does converge when the values at infinity are used for the linearized in-going characteristic variables in the x-direction, i.e.,

$$v(-0.25, y) = v_{-\infty} = 0.0$$
$$\bar{c}\rho(-0.25, y) + \bar{\rho}u(-0.25, y) = \bar{c}\rho_{-\infty} + \bar{\rho}u_{-\infty}$$
$$\bar{c}\rho(0.27, y) - \bar{\rho}u(0.27, y) = \bar{c}\rho_{\infty} - \bar{\rho}u_{\infty}.$$

The difference $\rho^{(I)} - \rho^{(T)}$, where $\rho^{(I)}$ is obtained in the last experiment is labeled I in Fig. 7. The error is obviously very large. It is even much larger than the error in the boundary data.

One could ask whether the large regions are large enough to give an accurate solution for comparison in the experiments presented above. One reason for that is the fact that the free stream values of at least two components of the solution are known in all the experiments. Besides, the experiments actually show that the boundary conditions have approximated the solution well in the area between the boundaries of the large and small regions.

8. CONCLUSION

The boundary conditions presented here lead to very accurate solutions even when the computational domain is made relativel small. They require Fourier transformations back and forth along the artificial boundary at every solution step. Assuming that the points are ordered in x, that is hardly a drawback in connection with Newton's method since the number of solution steps, and hence the number of Fourier transformations, is low. Most of the computational work at the boundary is devoted to Gauss eliminations at the corners of the Jacobian [6]. This work corresponds to that over just one extra grid line across the channel. The number of solution steps needed is not increased by the fundamental boundary conditions. The channel problem has been solved efficiently with Newton's method, and hence a

very efficient procedure is obtained when the fundamental boundary conditions are used to decrease the computational region in connection with Newton's method.

Time-dependent procedures require a much larger number of solution steps, and hence also a much larger number of Fourier transformations. Without using the FFT the work at the boundary corresponds to that over a fixed interval along the channel. The FFT makes the boundary conditions more efficient when the mesh is refined. Much work at the boundary can be saved by using fewer Fourier coefficients. The fundamental boundary conditions for the external problem are used in connection with a time-dependent procedure in [5].

ACKNOWLEDGMENTS

This work forms part of my doctoral dissertation. I want to express my deep gratitude to Professor Bertil Gustafsson for invaluable and encouraging guidance. The work has been supported financially by the Institute for Applied Mathematics, ITM, Stockholm, Sweden, and the Swedish Board for Technical Development.

REFERENCES

1. A. BAYLISS AND E. TURKEL, *J. Comput. Phys.* **48**, 182 (1982).
2. B. ENGQUIST AND A. MAJDA, *Math. Comput.* **31**, 629 (1977).
3. B. ENGQUIST AND A. MAJDA, *Commun. Pure Appl. Math.* **32**, 312 (1979).
4. L. FERM, Report 102, Department of Scientific Computing, Uppsala University, 1985 (unpublished).
5. L. FERM, Report 108, Department of Scientific Computing, Uppsala University, 1987 (unpublished).
6. L. FERM AND B. GUSTAFSSON, *Comput. Fluids* **10**, 261 (1982).
7. G. J. FIX AND S. P. MARIN, *J. Comput. Phys.* **28**, 253 (1978).
8. B. GUSTAFSSON, Manuscript Classic-87-16, Center for Large Scale Scientific Computation, Stanford University, 1987 (unpublished).
9. B. GUSTAFSSON AND H. O. KREISS, *J. Comput. Phys.* **30**, 333 (1979).
10. T. HAGSTROM AND H. B. KELLER, *SIAM J. Math. Anal.* **17**, 322 (1986).
11. T. HAGSTROM AND H. B. KELLER, *SIAM J. Sci. Statist. Comput.* **7**, 978 (1986).
12. D. RUDY AND J. C. STRIKWERDA, *Comput. Fluids* **9**, 327 (1981).